

# WIMP search from XMASS-I fiducial volume data with background prediction

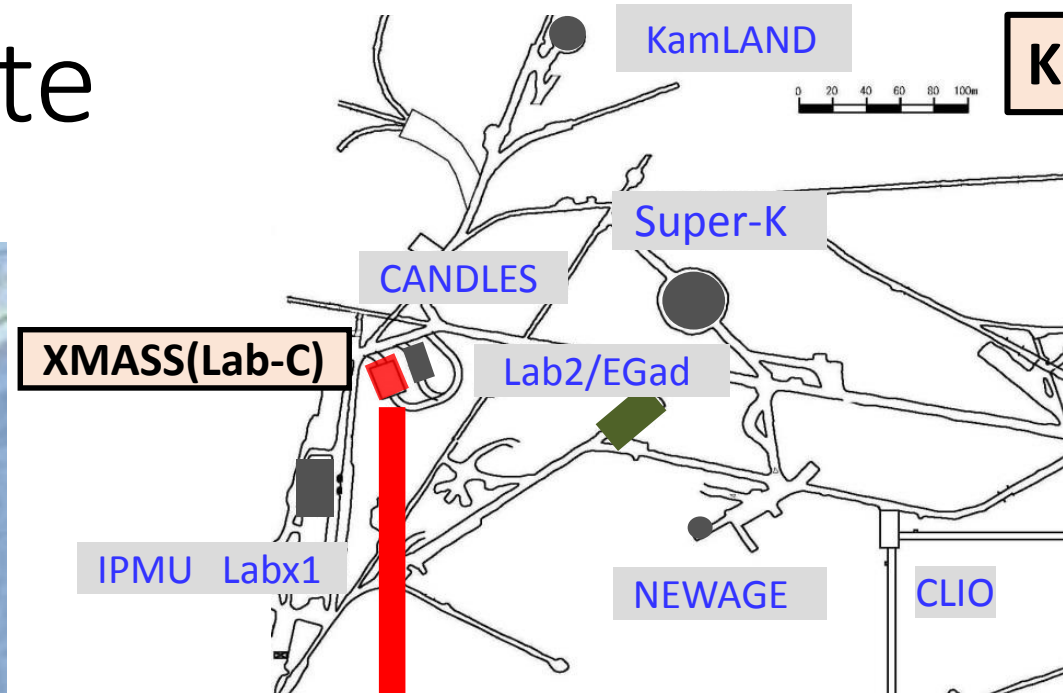
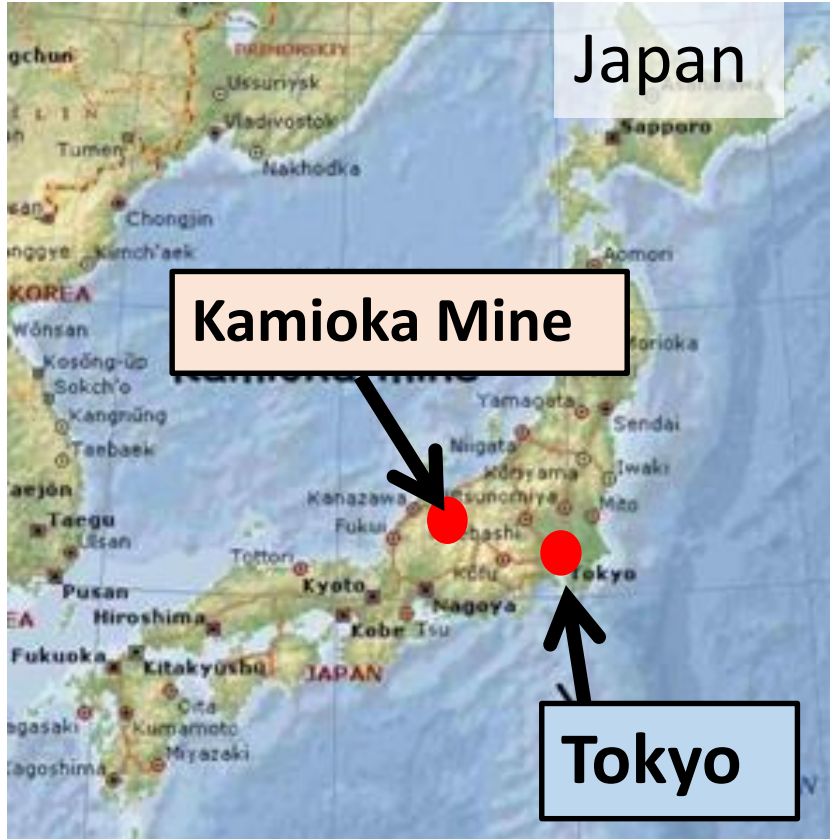
15<sup>th</sup> International Conference on Topics in Astroparticle  
and Underground Physics (TAUP 2017)

Jul. 24–28, 2017,  
Sudbury, ON, Canada

26<sup>th</sup> of Jul. 2017 (14:45–15:00)  
A. Takeda for the XMASS Collaboration

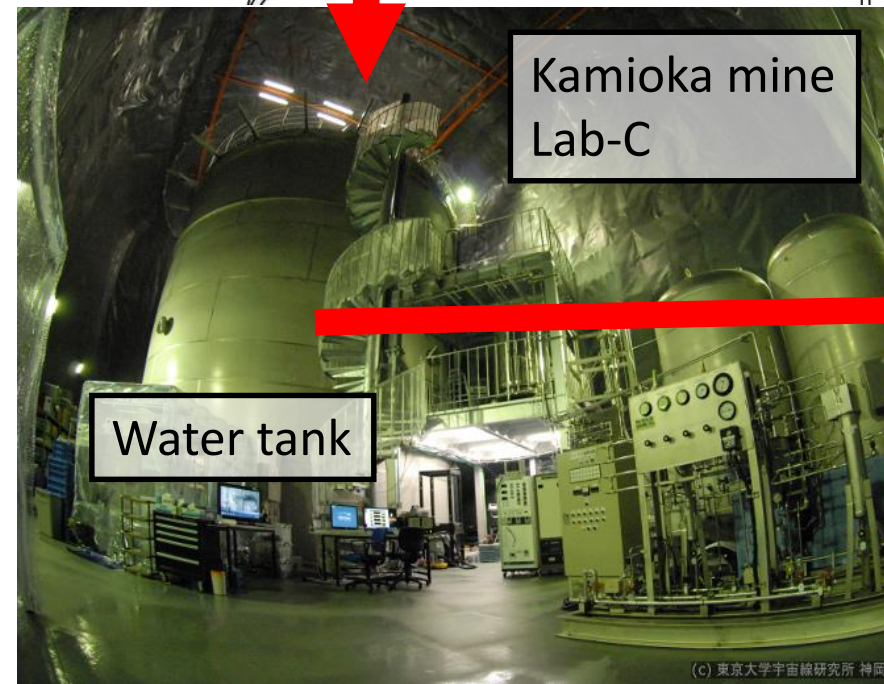


# Experimental site



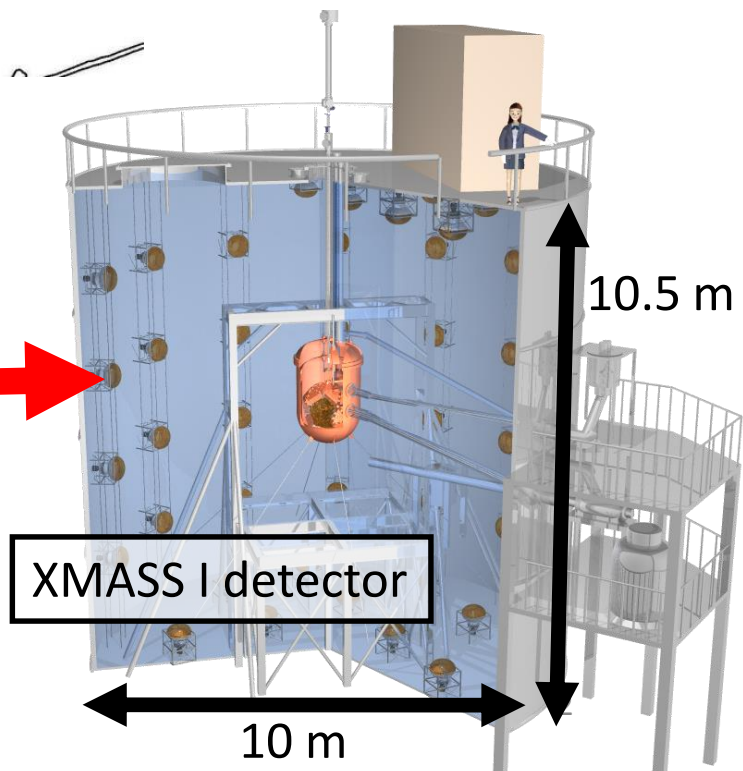
**Kamioka Mine**

~1000m underneath  
Mt. Ikenoyama.  
(2700 m.w.e.)



**Kamioka mine  
Lab-C**

**Water tank**



**XMASS I detector**

10.5 m  
10 m

(c) 東京大学宇宙線研究所 神岡

# XMASS-I detector

- **Inner detector**

- Single phase liquid xenon detector. (832 kg xenon for sensitive region)
- 642 low background PMTs. (2 inch, HAMAMATSU R10789)
  - each PMT signal is recorded by 10-bit 1GS/s waveform digitizers.
- High light yield:  $\sim 15$  PE/keV.

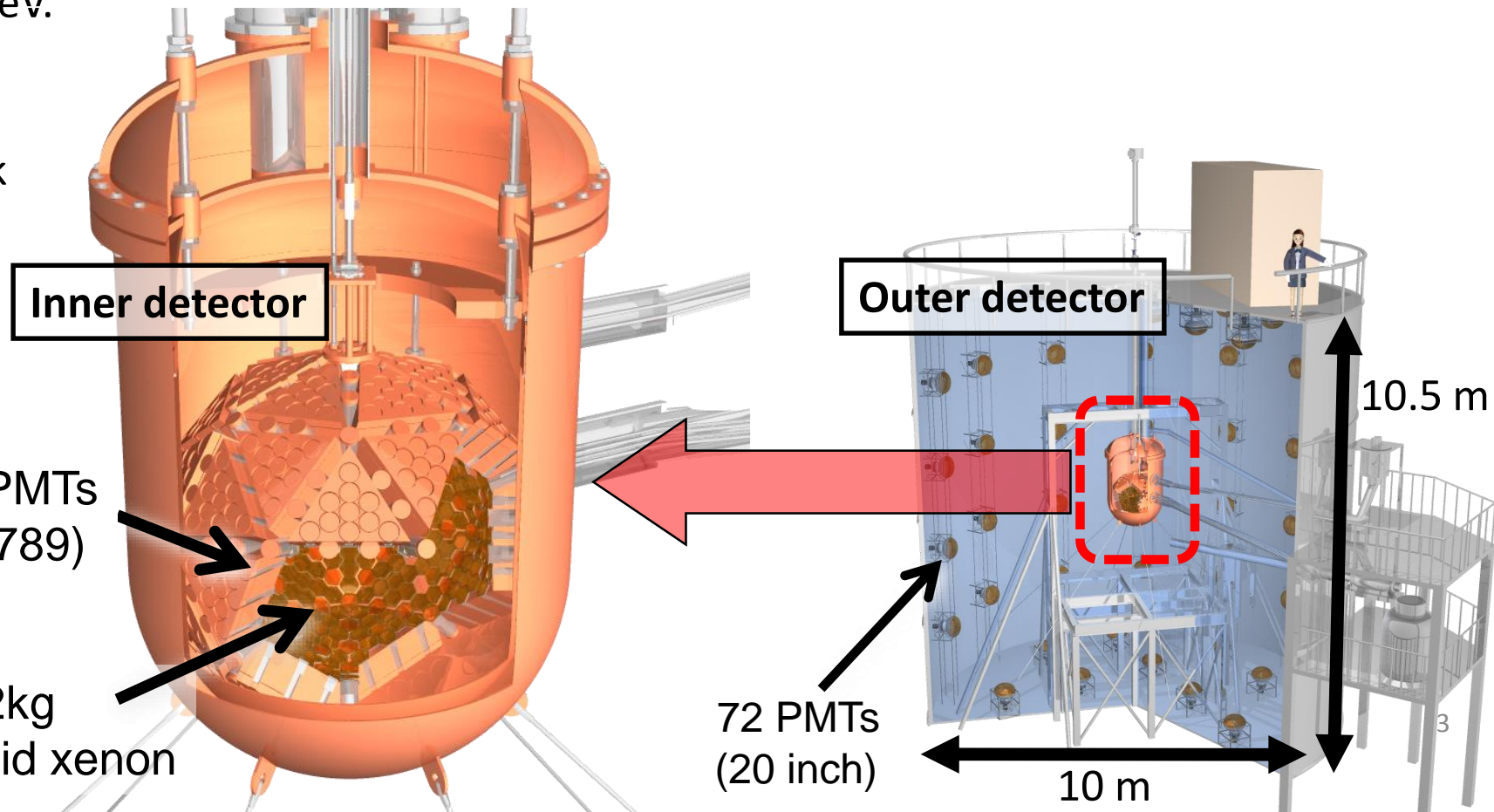
- **Outer detector**

- 10 m x 10.5 m water tank with 72 PMTs (20 inch) for active muon veto and passive radiation shield.



642 PMTs  
(R10789)

832kg  
liquid xenon



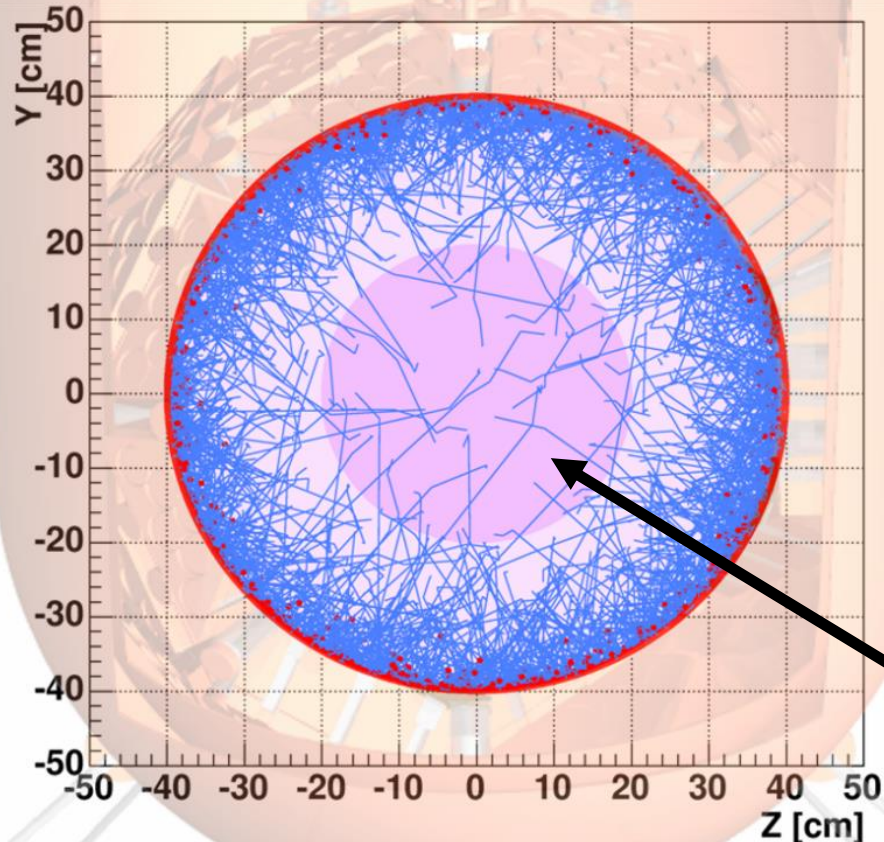
72 PMTs  
(20 inch)

10 m

10.5 m

# Self-shielding of $\gamma$ -ray background

Traces of U-chain gamma-rays from PMTs



- Owing to high atomic number ( $Z=54$ ), external gamma-ray background (mainly coming from PMTs) can be shielded by liquid xenon itself.
- By selecting events occurred in the restricted inner volume (fiducial volume) low background can be achieved.

Fiducial volume

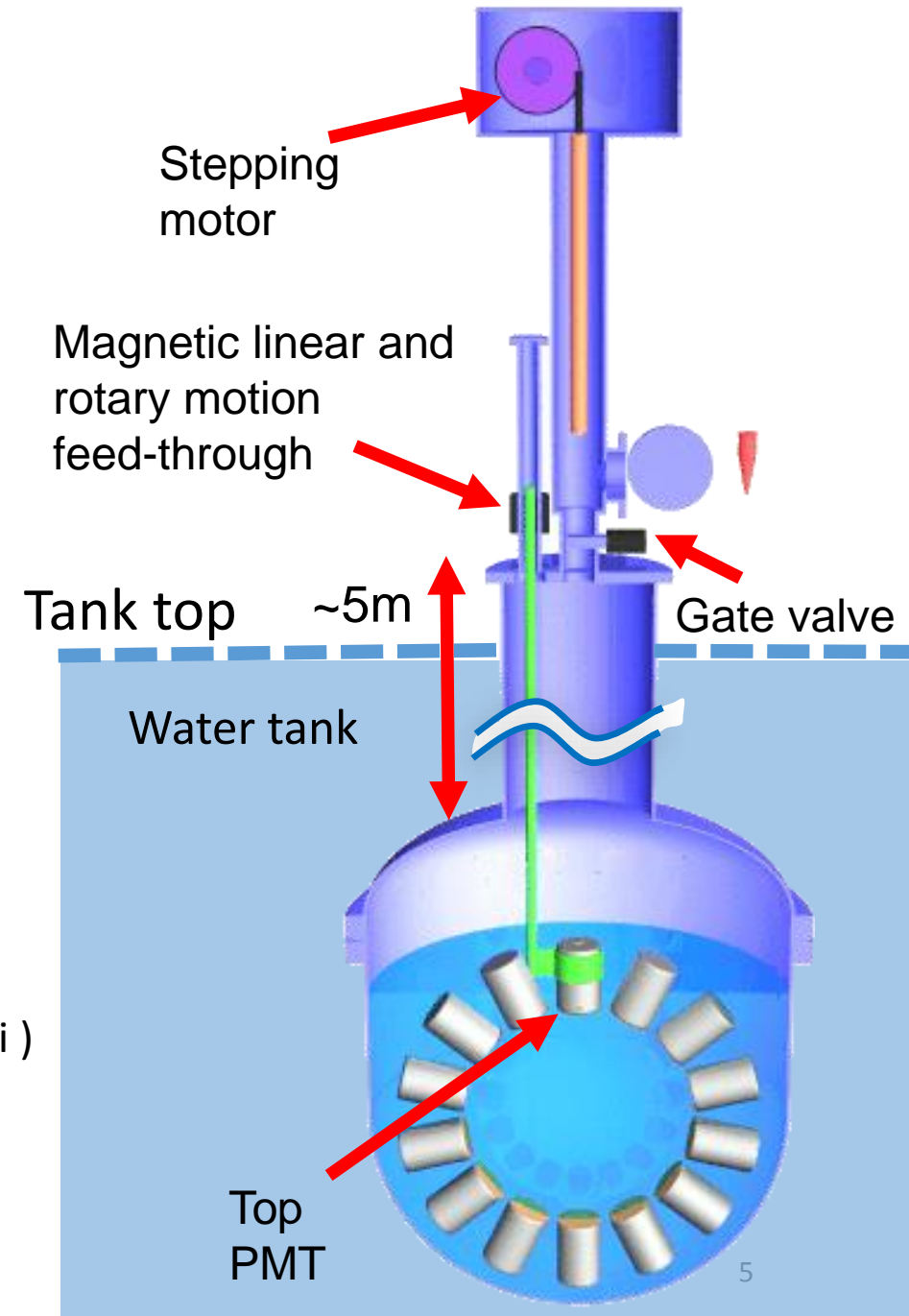
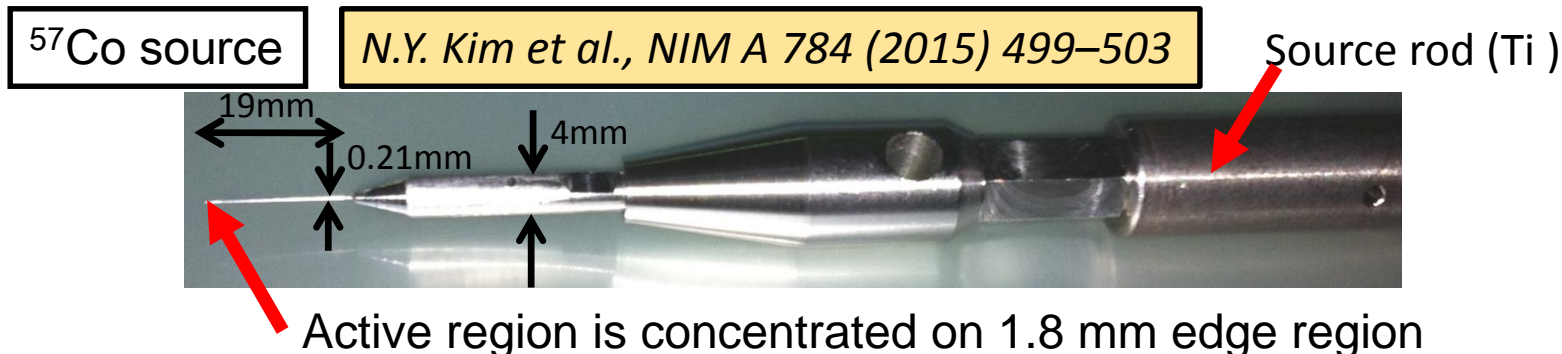
# Detector calibration

- Various RI sources can be inserted inside the sensitive volume w/o interrupting detector operation.
- Used for light yield monitoring, optical parameter tuning, energy and timing calibration etc.

RI	Energy [keV]	diameter [mm]	Geometry
(1) $^{55}\text{Fe}$	1.65(*1), 5.9	10	2pi source
(2) $^{109}\text{Cd}$	8, 22, 25, 88	5	2pi source
(3) $^{241}\text{Am}$	17.8, 59.5	0.17	2pi/4pi source
(4) $^{57}\text{Co}$	59.3(*2), 122	0.21	4pi source
(5) $^{137}\text{Cs}$	662	5	cylindrical

(\*1) 4.2 keV (averaged) L-shell X-ray escape from 5.9 keV K-shell X-ray.

(\*2) Tungsten K-shell X-ray used for detector housing.



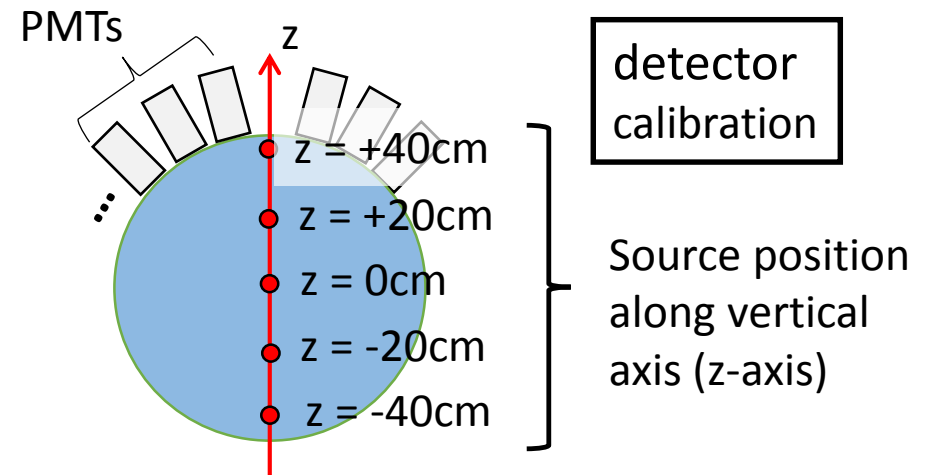
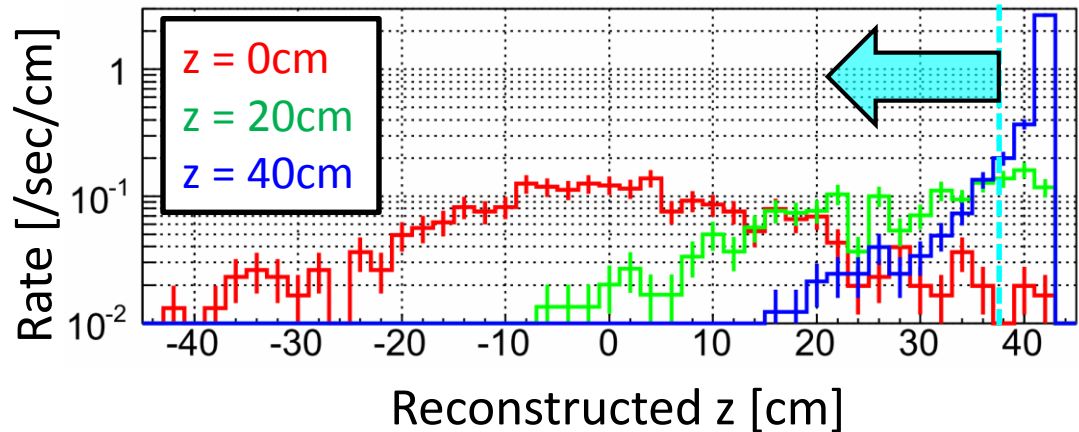
# Vertex reconstruction (based on timing, R(T))

- Using FADC hit timing of each PMT.
- Timing constant for 2–10 keV events:  $25 \pm 2$  ns.
- Position reconstruction is done by using likelihood method from probability density function for each PMT.

$$L(\vec{X}, T) = \prod_{i=1}^{N_{hits}} P\left(t_i - \frac{|\vec{x}_i - \vec{X}|}{v_g} - T\right)$$

$P(\tau)$  : probability density function  
 $x_i, t_i$  : PMT position and hit time  
 $v_g$  : group velocity in Lxe (110mm/ns)

$^{241}\text{Am}$  calibration data (5–10 keV)



→ Surface events  $> 38$  cm are effectively removed from this distribution.  
 $R(T) < 38$  cm selection is used for event reduction.

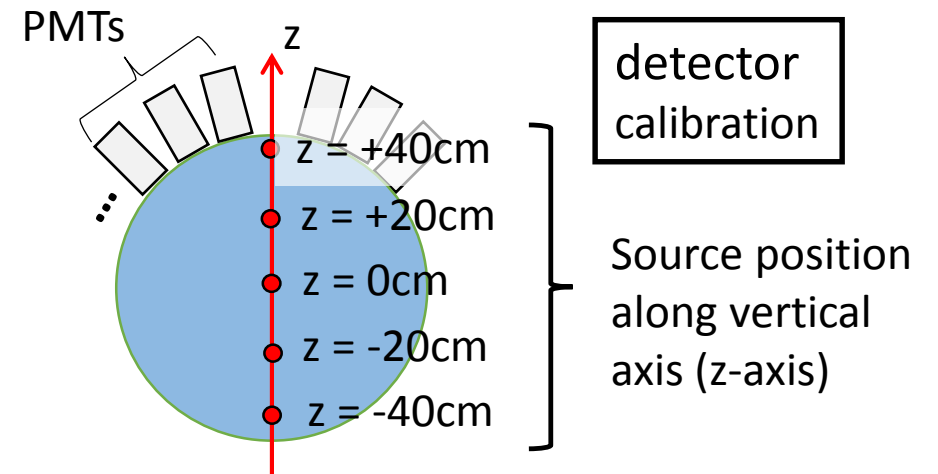
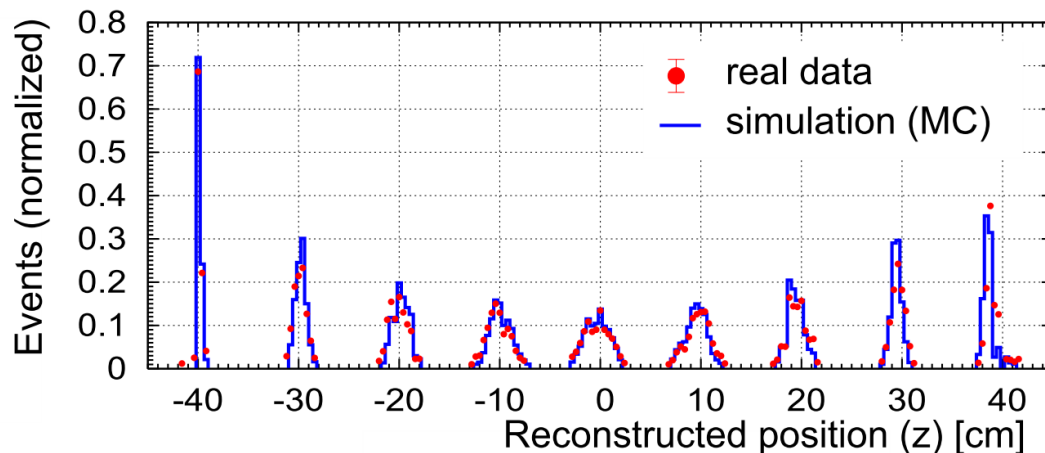
# Vertex reconstruction (based on photo electron, R(PE))

## ● Position reconstruction

- (1) Making acceptance map: Many grid points are defined inside whole detector volume including detector surface. Events are generated at each grid point and photo-electrons (pe) expected in each PMT are calculated by our MC.
- (2) From measured pe and scaled acceptance map ( $\mu$ ) in (1), position is calculated where following likelihood is maximum.

$$\log(L) = - \sum_{\text{PMT}} \log \left( \frac{\exp(-\mu) \mu^{\text{pe}}}{\Gamma(\text{pe} + 1)} \right) \quad \Gamma(x): \text{Gamma function} \\ (\Gamma(n) = (n-1)!, n > 0)$$

Reconstructed position distribution of  $^{57}\text{Co}$  events (122 keV)



# Evaluation of RI activities in XMASS-I (1/2)

- Based on RI screening for detector materials mainly with HPGe detector.
- RI activities are evaluated by spectrum fitting for  $> 400$  pe ( $\sim 30$  keV) between data and MC with constraints from screening results.



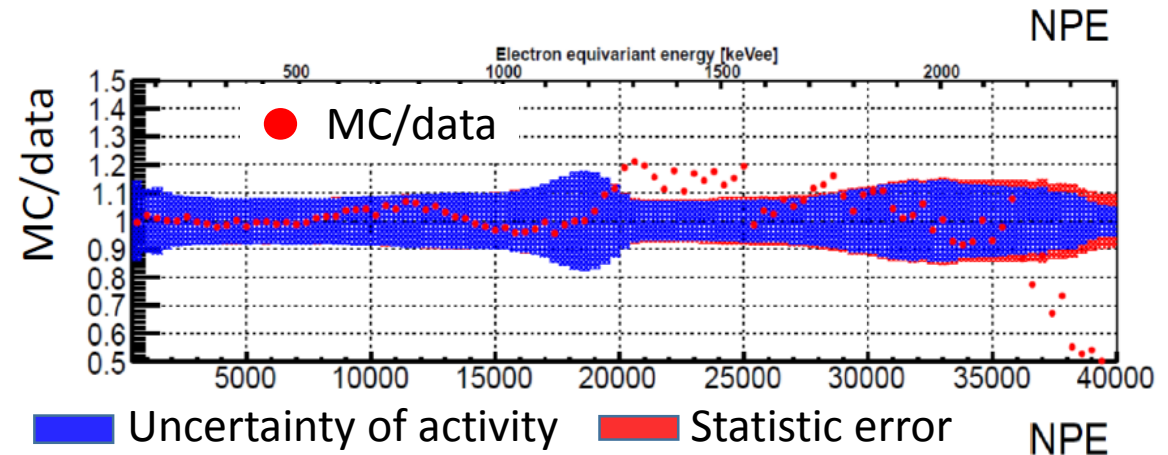
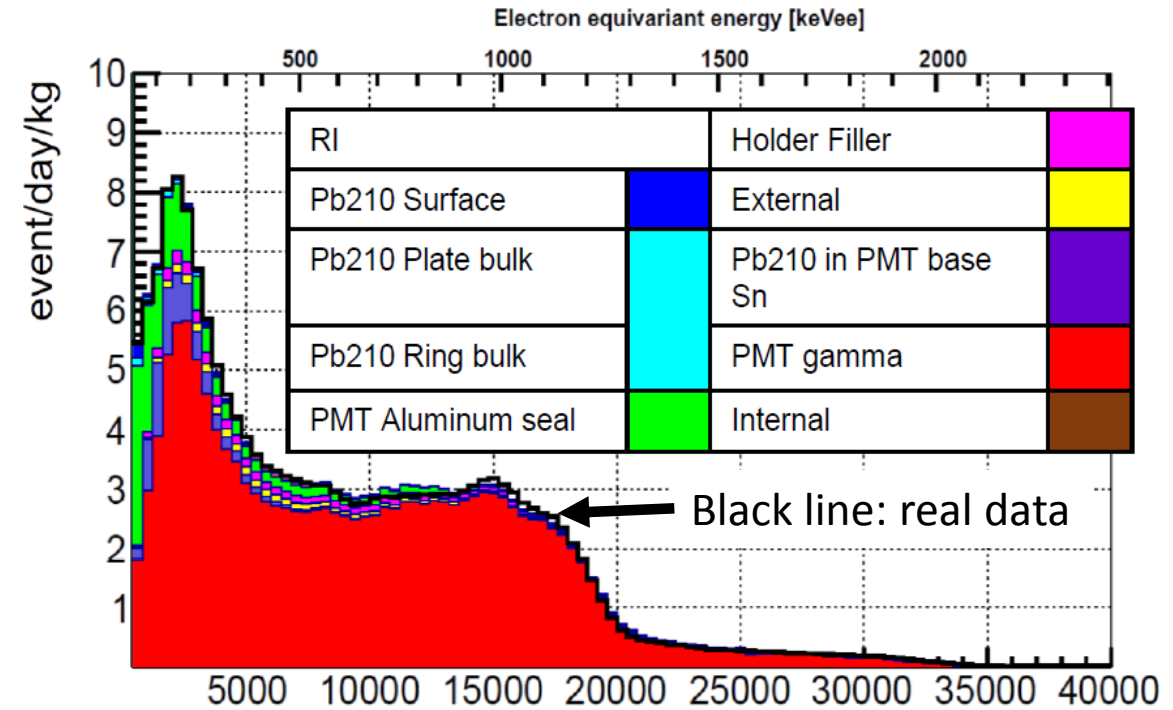
ex. RI screening results for PMT with HPGe detector.

- PMT aluminum seal

	Bq
$^{238}\text{U}$ – $^{230}\text{Th}$	$1.5 \pm 0.4$
$^{210}\text{Pb}$	$2.85 \pm 1.15$
$^{232}\text{Th}$	$0.096 \pm 0.018$
$^{235}\text{U}$ – $^{207}\text{Pb}$	$\sim 1.5 \times 4.5\%$

- PMT + base (whole measurement)

	mBq/PMT
$^{232}\text{Th}$	$1.80 \pm 0.31$
$^{238}\text{U}$	$2.26 \pm 0.28$
$^{210}\text{Pb}$	$200 \pm 100$
$^{60}\text{Co}$	$2.92 \pm 0.16$
$^{40}\text{K}$	$9.10 \pm 2.15$

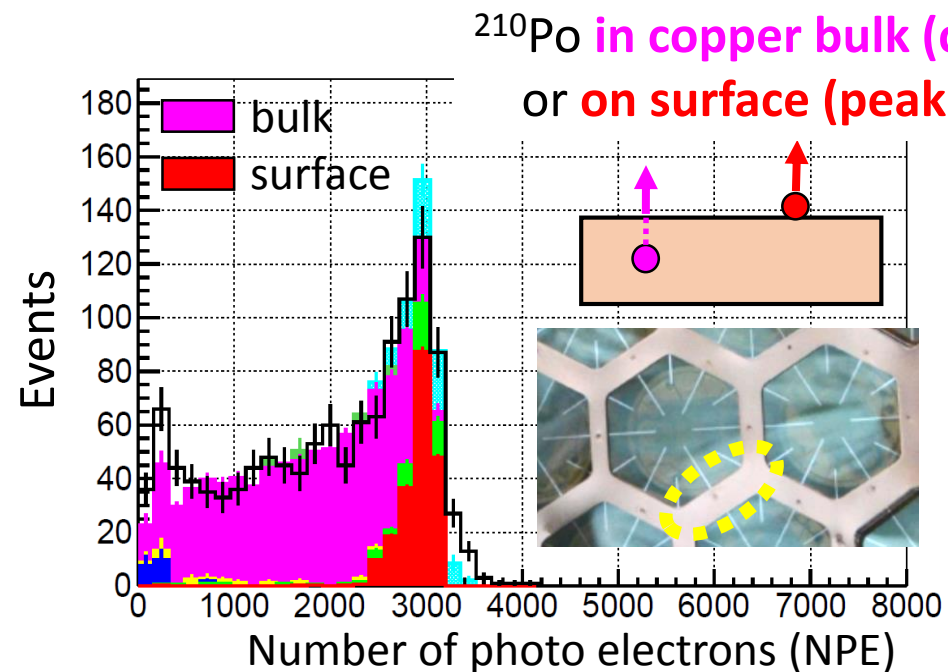




# Evaluation of RI activities in XMASS-I (2/2)

## ● $^{210}\text{Pb}$ in copper surface and bulk

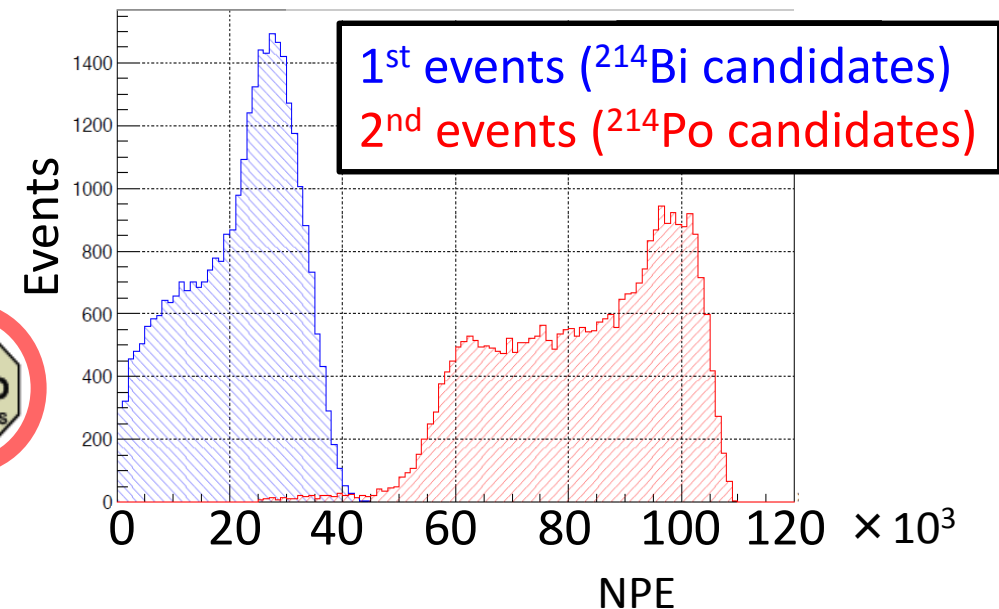
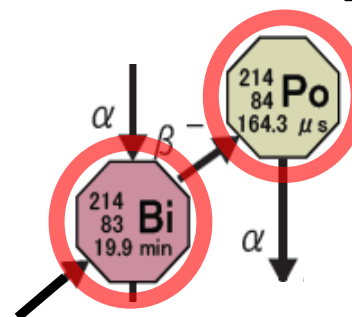
- $\alpha$  events selection from scintillation decay time.
- $^{210}\text{Pb}$  in copper surface/bulk were estimated from shape of energy spectrum caused by  $^{210}\text{Po}$   $\alpha$  decay.
- $^{210}\text{Pb}$  in the bulk of OFHC copper was also measured independently by a low background  $\alpha$ -particle counter. (XIA Ultra-Lo-1800)



## ● RI in liquid xenon

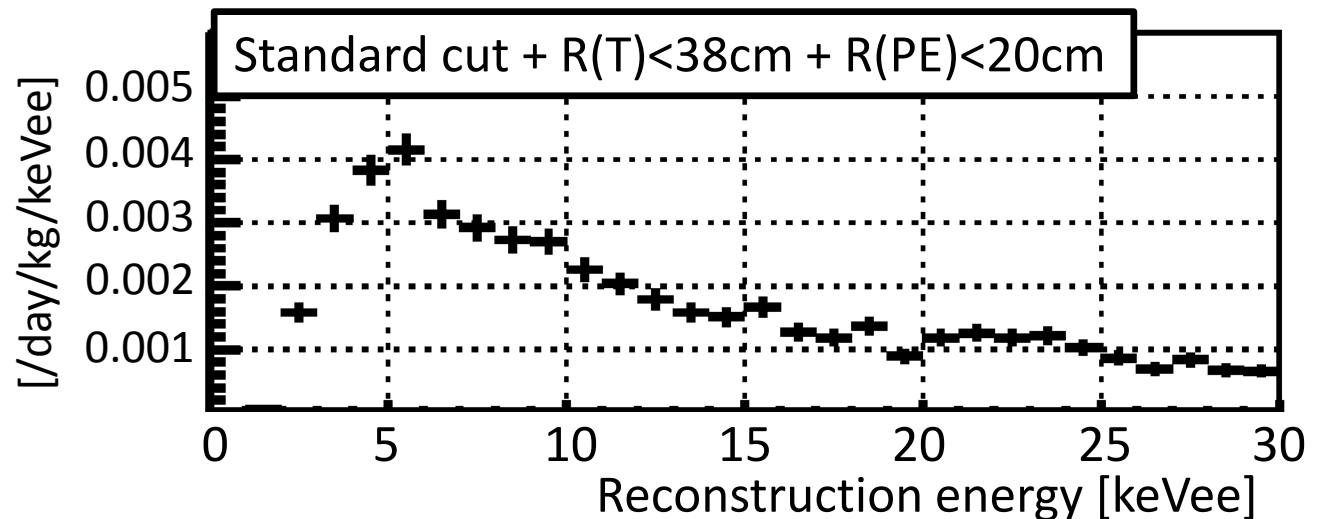
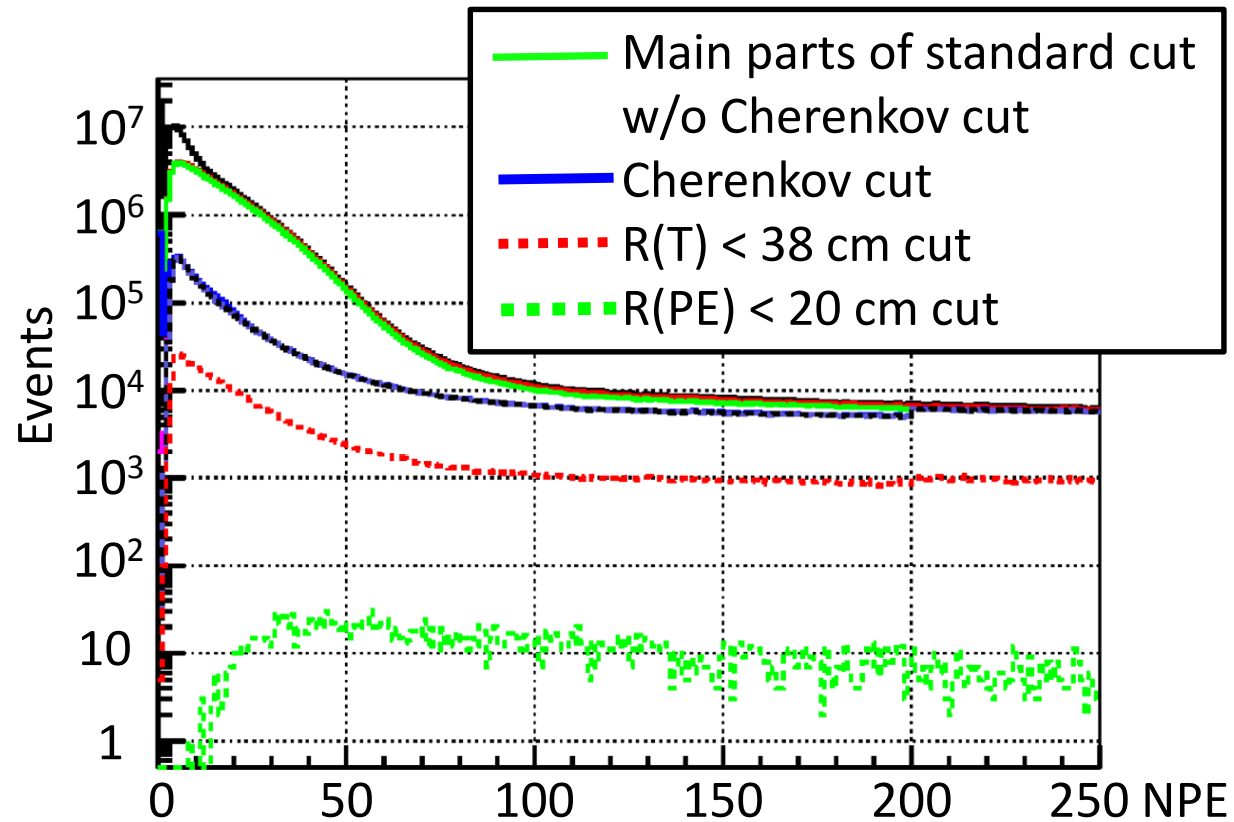
- Coincidence analysis was used.
  - $^{222}\text{Rn}$ :  $^{214}\text{Bi} - ^{214}\text{Po}$  (164  $\mu\text{s}$ )
  - $^{85}\text{Kr}$ :  $\beta - \gamma$  (1.015  $\mu\text{s}$ , 0.343%)
- $^{14}\text{C}$  and  $^{39}\text{Ar}$  were estimated from spectrum fitting.

Down stream  
of  $^{222}\text{Rn}$



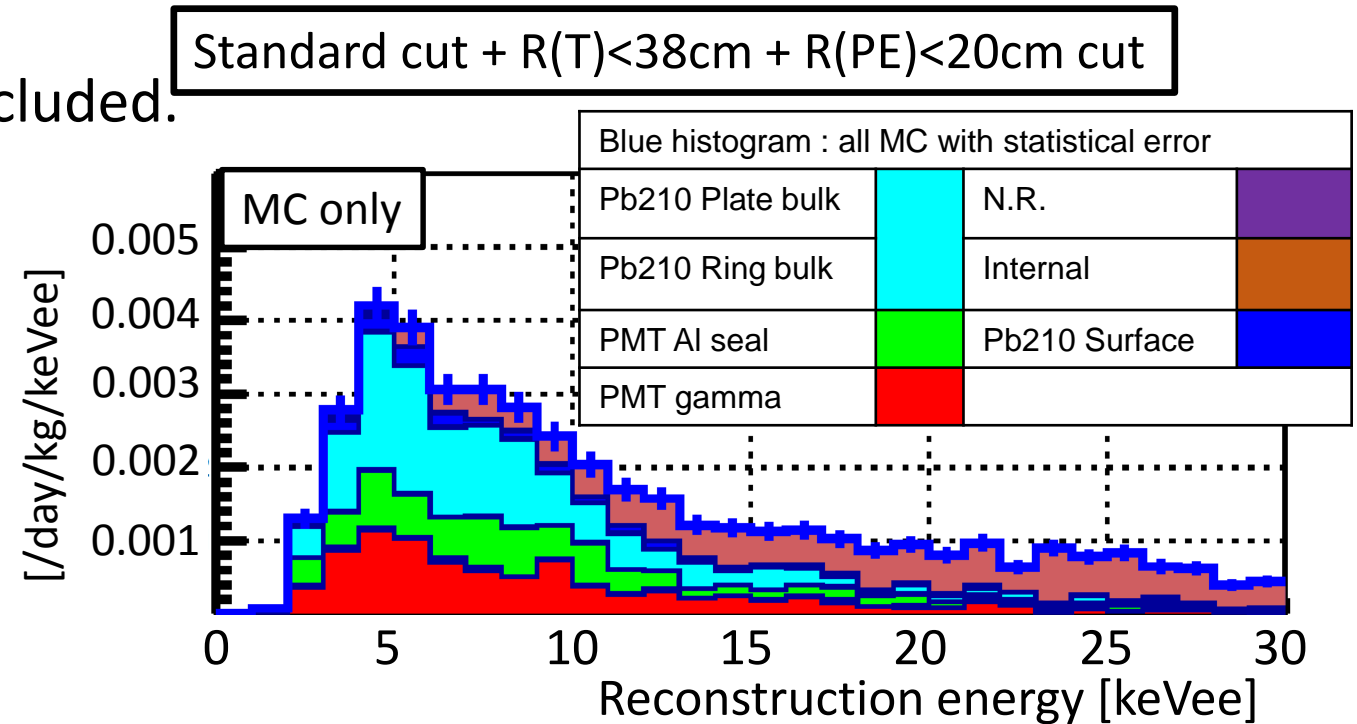
# Data reduction

- **Live time:** 705.88 days  
2013/Nov. /20 – 2016/Mar./29
- **Standard cut:**
  - Reduction of Cherenkov event is effective.  
Main origin of Cherenkov events is  $\beta$ -ray in PMT quartz window emitted from  $^{40}\text{K}$  in PMT photo-cathode.
- **R(T) < 38 cm and R(PE) < 20 cm cuts** give another  $O(10^{-3})$  reduction.
- **Event rate after applying all cuts:**  
 $\sim 4 \times 10^{-3}$  /day/kg/keVee  
@5–5.5 keVee  
(signal efficiency:  $\sim 30\%$ )



# Background prediction with MC

- XMASS MC based on Geant4.
  - Detail detector geometry and responses of PMT and DAQ were included.
  - Optical parameters of LXe were traced with our periodical calibration ( $^{57}\text{Co}$  and  $^{60}\text{Co}$ ).
  - RI activities for each material were implanted.
  - Same live time as that of data.
  - Same reduction as that for data was applied.

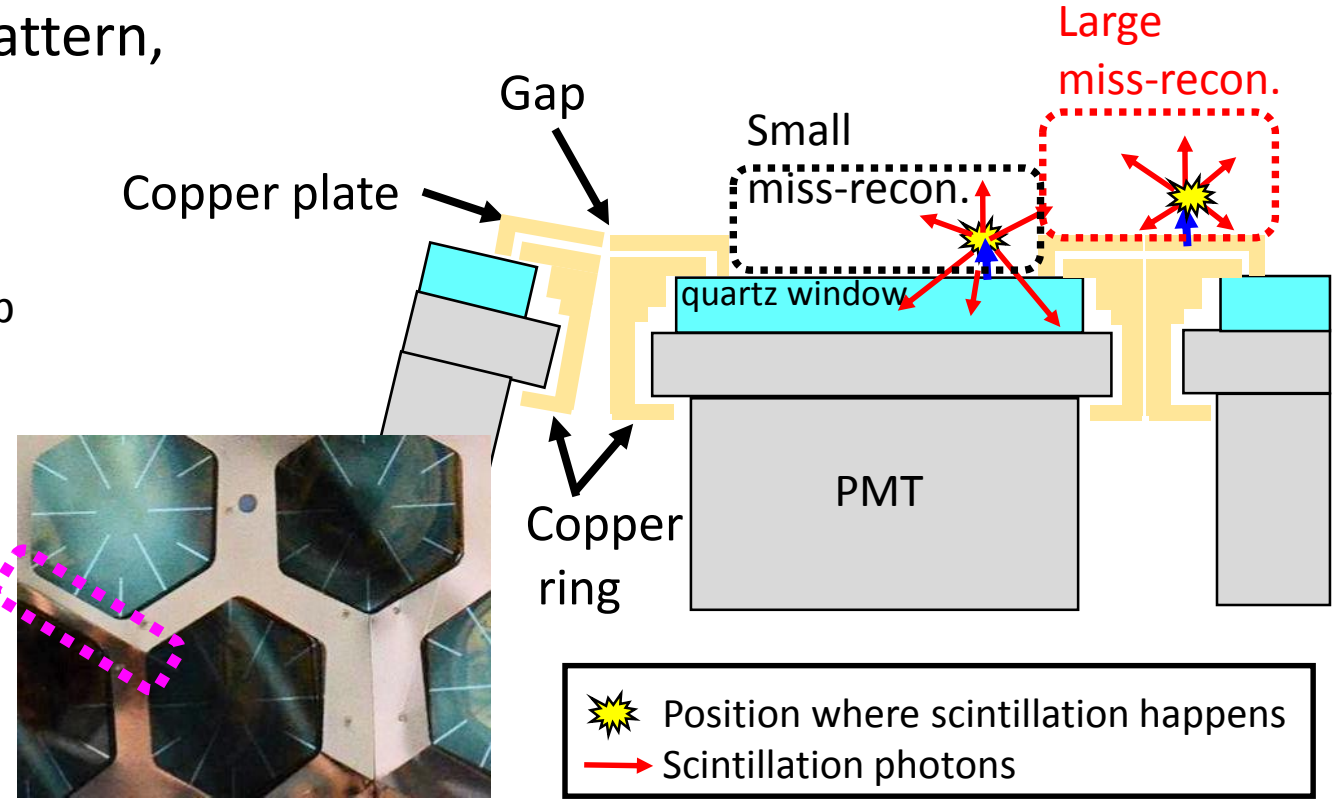
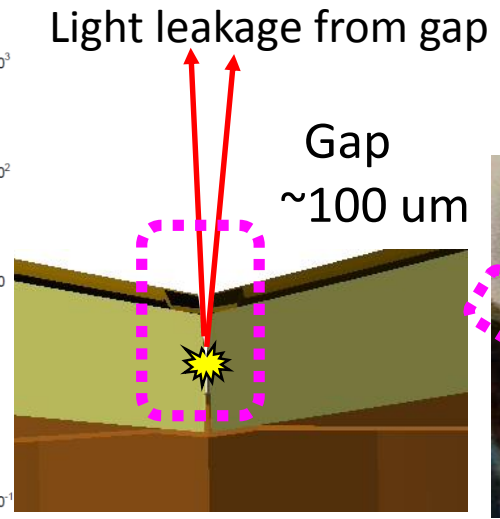
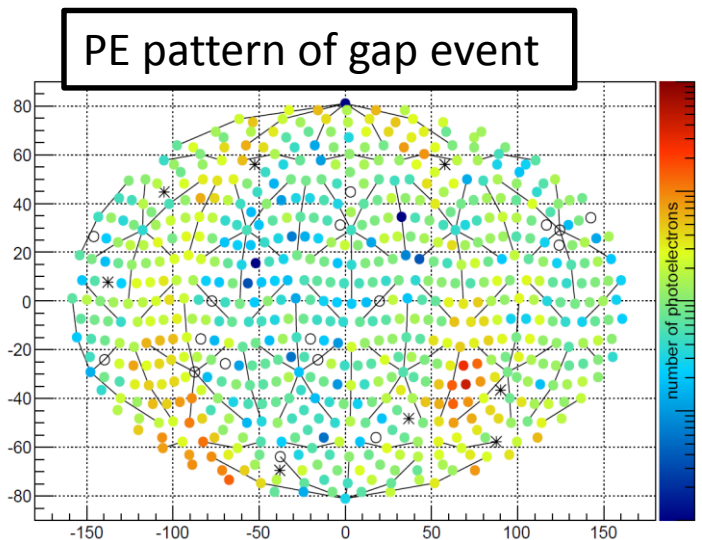
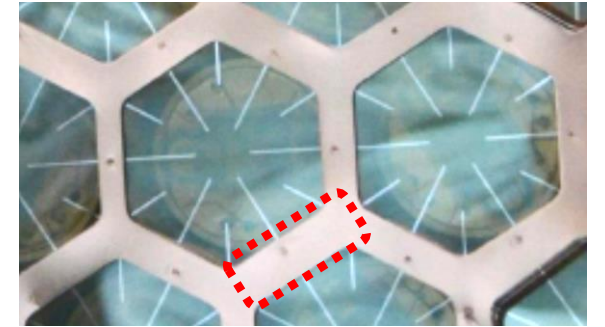


➔ Main BG origin is not internal but detector surface events (miss-reconstructed events).

# Miss-reconstructed events

- Events occurring on surface of copper plate are wrongly reconstructed to inside of the fiducial volume with some probabilities because closest PMT has small solid angle for these events.
- Light leakage from a gap around boundary between plate and plate makes special pattern, but, sometimes wrongly reconstructed inside the fiducial volume.

Structure around PMT



# Systematic error evaluation

All the possible systematic errors were evaluated

- **Related to surface condition:** it mainly affects to miss-reconstruction rate.
  - (1) Geometry of gap between plates coming from installation accuracy of plates.
  - (2) Roughness of ring surface inside the gap.
  - (3) Reflection of plate surface.
  - (4) Floating of plate coming from installation accuracy of each plate.
- (5) Geometry and property of aluminum seal
- (6) Related to reconstruction: grid dependency and rate of miss-reconstruction.
- (7,8) Uncertainty for scintillation decay time and response of PMT.
- (9) Optical parameters of LXe.
- (10) Effect of dead PMTs (10 dead PMTs exist)
- (11) for  $^{206}\text{Pb}$  recoil from  $^{210}\text{Po}$   $\alpha$  decay on copper surface.

Contents	Systematic error	
	2-15 keVee	15-30 keVee
(1) Plate gap geometry	+6.2/-22.8%	+1.9/-6.9%
(2) Ring roughness	+6.6/-7.0%	+2.0/-2.1%
(3) Cu ref dependence	+5.2/-0.0%	+2.5/-0.0%
(4) Plate floating	+0.0/-4.6%	+0.0/-1.4%
(5) Al seal dependence	+0.7/-0.7%	+0.0/-0.0%
(6) Reconstruction	+3.0/-6.2%	+0.0/-0.0%
(7) Timing (decay time, TTS)	+4.6/-2.9%	+0.4/-5.3%
(8) Timing (response in detector surface)	+0.0/-8.0%	+0.0/-0.0%
(9) Absorption & scattering	+0.7/-6.7%	+1.5/-1.1%
(10) Dead tube origin	+10.3/-0.0%	+45.2/-0.0%
(11) N.R.	+0.7/-0.7%	+0.0/-0.0%

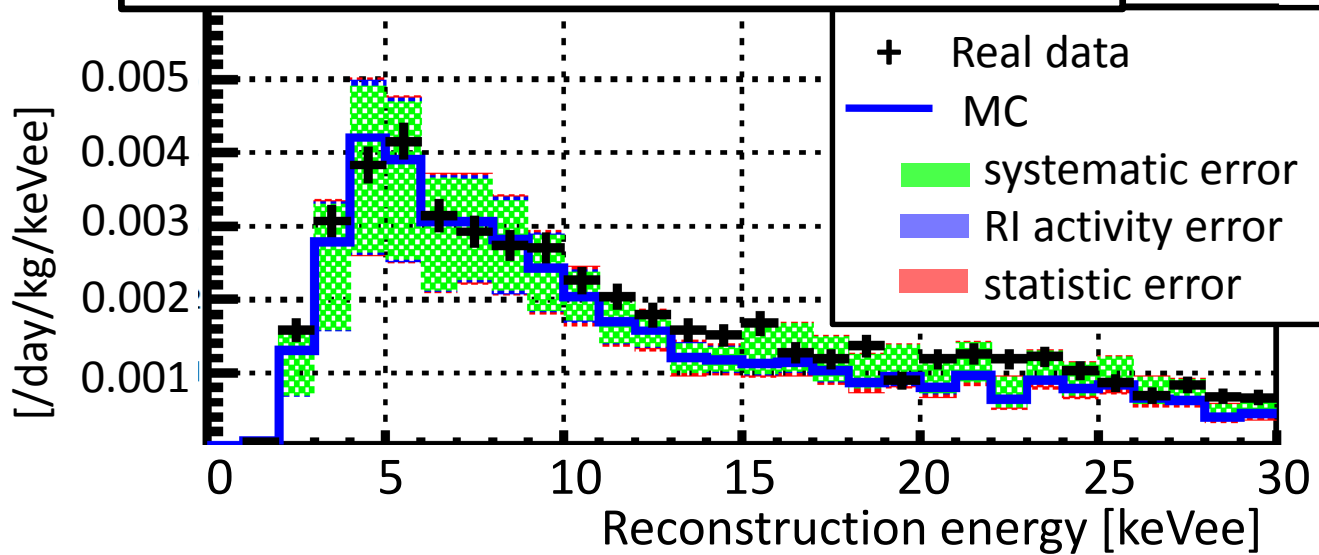
# Systematic error evaluation

All the possible systematic errors were evaluated

- **Related to surface condition:** it mainly affects to miss-reconstruction rate.
  - (1) Geometry of gap between plates coming from installation accuracy of plates.
  - (2) Roughness of ring surface inside the gap.
  - (3) Reflection of plate surface.
  - (4) Floating of plate coming from installation accuracy of each plate.

Contents	Systematic error	
	2-15 keVee	15-30 keVee
(1) Plate gap geometry	+6.2/-22.8%	+1.9/-6.9%
(2) Ring roughness	+6.6/-7.0%	+2.0/-2.1%
(3) Cu ref dependence	+5.2/-0.0%	+2.5/-0.0%
(4) Plate floating	+0.0/-4.6%	+0.0/-1.4%
(5) Al seal dependence	+0.7/-0.7%	+0.0/-0.0%
(6) Reconstruction	+3.0/-6.2%	+0.0/-0.0%
(7) Timing (decay time, TTS)	+4.6/-2.9%	+0.4/-5.3%
(8) Timing (response in detector surface)	+0.0/-8.0%	+0.0/-0.0%
(9) Absorption & scattering	+0.7/-6.7%	+1.5/-1.1%
(10) Dead tube origin	+10.3/-0.0%	+45.2/-0.0%
(11) N.R.	+0.7/-0.7%	+0.0/-0.0%

Standard cut + R(T)<38cm + R(PE)<20cm cut



← Real data is well explained with background MC.

# WIMP search with background evaluation in fiducial volume

- 705.88 live days data applying fiducial volume data reduction were used. (standard +  $R(T) < 38\text{cm}$  +  $R(PE) < 20\text{cm}$  cut)
- Energy spectrum of data was fitted with background MC and WIMP MC in the energy range of 2–15 keVee considering systematic error in both background and WIMP MC.
- Best fit result is consistent with no WIMP case, then 90% C.L. upper limit on the WIMP-nucleon cross section was derived.
- Our preliminary limit is  $2.2 \times 10^{-44} \text{ cm}^2$  for 60 GeV WIMP mass.

